Journal of Undergraduate Chemistry Research, **2021**,20 (3), 63

AGGREGATION-INDUCED EMISSION FROM 1- AND 2-ETHYLNAPHTHALENE-BIPHENYL EXCIPLEXES FROM SELF-ASSEMBLED VAN DER WAALS COMPLEXES BY VAPOR DEPOSITION ON Al_2O_3

Samantha C. Rosenhagen*, Cassidy C. Tran* and A.M. Nishimura†

Department of Chemistry, Westmont College, Santa Barbara, CA 93108

Abstract

By vapor deposition on liquid nitrogen cooled crystal of Al_2O_3, bilayers of each of the isomers of ethylnaphthalene were formed with biphenyl. Temperature programmed desorption (TPD) experiments were then performed. The self-assembly due to the van der Waals complexation yielded fluorescence intensity with λ_{max} at 324 nm. The fluorescence that was observed during the TPD was compared to spectral signatures of multilayer ethylnaphthalene and biphenyl and the fluorescence of the exciplex was determined to be that of the ethylnaphthalene. During the TPD, the disorder-to-order transition of biphenyl caused a change in the fluorescence intensity of the exciplex. Plots of the intensity of the exciplex as a function of the ratio of the coverages of biphenyl to 2- and 1-ethylnaphthalene showed the stoichiometry of the exciplex was approximately 7±1:1 and 4±1:1, respectively. From mass specific TPD data, the van der Waals energies were determined to be approximately 3.2±0.5 kJ mol^{-1} for the two complexes.

†corresponding author: nishimu@westmont.edu

Keywords:1-ethylnaphthalene, 2-ethylnaphthalene, biphenyl, exciplex, van der Waals, aggregation-induced emission, self-assembly

Introduction

Two decades ago, the term aggregation-induced emission was used to describe enhanced emission from molecules that otherwise exhibited quenching via non-radiative pathways due to rotational or vibrational modes (1-5). Dimishing or eliminating this quenching was accomplished by rigidly holding these groups in place by steric hindrance, covalent/ionic bonding or van der Waals interaction (1-5). To date, examples of aggregation-induced emission are restricted to large molecules or biomolecules (1-5). In order to model aggregation-induced emission at the simplest level, biphenyl was chosen because it can exist in a planar of twisted conformation depending on rotation about the C-C bond and result in planar and twisted conformations. Furthermore van der Waals interactions with substituted naphthalenes can be used to impede the rotation about the single bond in biphenyl. Van der Waals clusters of this type have been observed with substituted naphthalenes (6)

The C-C rotational barrier of ethane is 2.029 kJ mol^{-1} (7-8) due to steric repulsion in the eclipsed conformation (9-10) and the hyperconjugation of the staggered conformation (11-12). Analogous effects exist for biphenyl. In vapor deposited biphenyl, analysis of the fluorescence spectra of the condensed phase revealed that the planar conformer was approximately 22 kJ mol^{-1} more stable than the twisted conformer (13-15), and hence either conformer is within the range of the van der Waals interaction that would be possible with ethylnaphthalene.

The advantage of biphenyl as the choice of the simplest model for aggregation-induced emission is that the spectral profiles of several substituted biphenyls in which the biphenyl framework was in the planar and out-of-plane are known. This allowed for the identification of the conformer of biphenyl (15-16). In the gas phase the conformer is known to have a dihedral angle at 45^o (17). Since vapor deposition of biphenyl is done from the gas phase, the λ_{max} ~ 320 nm fluorescence that was observed at deposition on Al_2O_3 was assigned to the conformer that is twisted. When biphenyl was vapor deposited or annealed at 160 K, the fluorescence red-shifted to λ_{max} ~ 340 nm and this emission has been assigned to the planar conformation (15-16) which is the geometry of biphenyl in the crystalline state (18). This conformation maximizes the electron delocalization in the phenyl groups (19). When vapor deposited at 138 K on Al_2O_3, the amorphous planar conformer predominate and λ_{max} further red-shifts to ~ 370 nm (15,16) and has been assigned to the biphenyl excimer with a planar geometry (15,16).

In addition, epitaxially, biphenyl is known to be sensitive to the surface morphology of the underlayer and the conformer of biphenyl as an overlayer will vary, depending on the nature of this underlayer (15). In a previous study (16), the planar conformer of biphenyl formed when deposited on a naphthalene underlayer and when optically excited, the fluorescence was exciplexial. The stoichiometry of the exciplex was found to be one molecule of naphthalene per molecule of biphenyl (22). Since the two molecules in the complex desorbed together when heated, the strength of the van der Waals complex between naphthalene and biphenyl was estimated to be about 5.5±0.5 kJ mol^{-1} (22). Also in a previous work, the van der Waals complexes and the resulting exciplexes of biphenyl with 1- and 2-methylnaphthalene were examined. For these, the van der Waals energies were reported to be 2.6±05 and 4.3±0.5 kJ mol^{-1}, respectively (25). In this study, further investigation into the exciplex formed by the two isomers of ethylnaphthalene with biphenyl is reported.

Experimental

High purity biphenyl and ethylnaphthalenes were purchased from commercial sources (Sigma-Aldrich, St. Louis, MO). These compounds were individually placed in 3 separate sample holders, outgassed and introduced into the ultra-high vacuum chamber with background base pressure of 1 x 10^{-9} Torr for molecular hydrogen. Deposition onto a single crystal of Al_2O_3 (0001) (Crystal Systems, Inc., Salem, MA) was done by using one of the precision leak valves. The substrate was suspended on the end of a liquid nitrogen cryostat via copper post on either side of the Al_2O_3 with a sapphire spacer for electrical and thermal isolation. TPD experiments were done by resistively heating the Al_2O_3 crystal and adjusting the current through a Ta foil. In addition to the Ta foil, a

type K thermocouple was in thermal contact with the Al_2O_3 crystal.

Details of the experimental set up have been previously published (21) and only a brief outline is given. An Ocean Optics USB4000 spectrometer (Ocean Optics, Dunedin, FL) was used to obtain the fluorescence spectra. During the TPD, a LabVIEW (National Instruments, Austin, TX) program that had been written in-house took the fluorescence spectra from an Ocean Optics USB4000 spectrometer (Ocean Optics, Dunedin, FL) in real time. The program simultaneously monitored the surface temperature of the Al_2O_3 crystal, and through a PID (proportional-integral-derivative) feedback algorithm, linearly ramped the temperature of the Al_2O_3 crystal at 2K s^{-1}. The program also scanned the residual gas analyzer for the masses of the compounds that had been deposited on the Al_2O_3. Manipulation of the very large numerical array of spectra as a function of temperature by a MATLAB (Mathworks, Natick, MA) template yielded the wavelength resolved TPD that are shown in Figures 1-6. To ensure a clean surface, the Al_2O_3 was heated to 300 K after each run.

The activation energy for desorption, E_a, was calculated by Redhead analysis in which a first-order desorption kinetics as described by King was assumed. The analysis is based on the mass spectral peak desorption temperature, T_p (26-28). The uncertainties in the desorption temperatures and the propagated error in the activation energies were ± 2%.

The surface coverages, Θ, in monolayers (ML) were calculated by calibrating the integrated mass spectral peaks to an optical interference experiment. The interference experiment yielded accurate rate of deposition with coverage error of ± 30%, and is described in detail elsewhere (21).

Annealing experiments involved the ramping of the temperature after deposition to a specified temperature. The specified temperature was held to within ±1 K for a set duration. Then the temperature was allowed to return to that at deposition.

Results and Discussion

Biphenyl:

The peak desorption temperature, T_p, of neat biphenyl was 234 K. First-order desorption was assumed and the activation energy for desorption, E_a, was calculated to be 60.8 kJ mol^{-1} (26-28). Upon deposition on Al_2O_3, electronic excitation of biphenyl exhibited fluorescence with a λ_{max} of 320 nm that has been previously assigned to the twisted conformer (15-16). (Figure 1). The adlayer underwent a disorder-to-order transition at 160 K, where λ_{max} red-shifted to 340 nm and has been assigned to the planar conformer of biphenyl (15-16).

2- and 1-ethylnaphthalene:

The peak desorption temperature from mass spectra of 2-ethylnaphthalene was 219 K and E_a was calculated to be 56.5 kJ mol^{-1} by assuming a first-order desorption kinetics (26-28). Vapor deposition of aromatic molecules typically results in an adlayer that is morphologically amorphous. In addition, when optically pumped, planar aromatic molecules such as ethylnaphthalene form excimers, or excited state dimers that exist only briefly (14) and the emission is characterized by a red-shift and broad spectrum compared to the monomer. The planar naphthalene group dictate the principal emissive property of the ethylnaphthalenes.

When the surface was heated in a TPD experiment, the amorphous adlayer of 2-ethylnaphthalene underwent a disorder-to-order transition, whereupon the fluorescence evolved to the monomer emission that was blue-shifted. Sufficient order existed so that the vibrational fine structure due to the C-H bending motion was resolved at 324 and 334 nm (23-24) as shown in Figure 2. This blue-shift in λ_{max} from excimer to molecular fluorescence for ethylnaphthalenes correspond to ~ 50 kJ mol^{-1} of energy (23-24).

From mass spectral data, T_p for 1-ethylnaphthalene was 216 K with a E_a of 55.7 kJ mol^{-1}. The wavelength-resolved TPD with a temperature ramp of 2 K s^{-1} for multilayer 1-ethylnaphthalene in Figure 3 shows a slight red-shift of about 4.$_5$ nm from 396 nm that begins at about 170 K. Surpringly, the disorder-to-order transition that typically was observed for naphthalene-type molecules could not be detected. However, when the temperature ramp rate was decreased from the usual 2 K s^{-1} to 0.5 K s^{-1}, the molecular fluorescence began to emerge and grew to the maximum intensity when the temperature was ramped at 0.25 K s^{-1}. Hence, for 1-ethylnaphthalene, the disorder-to-order transition is kinetically driven.

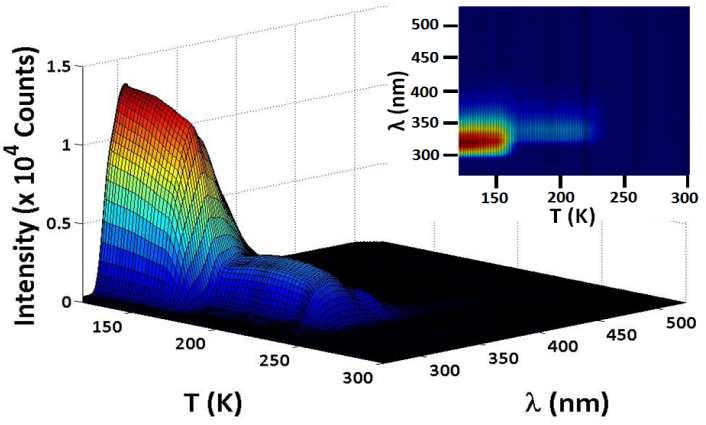

Figure 1. Wavelength-resolved TPD of multilayer biphenyl. $\Theta_{biphenyl}$ = 93 ML. Biphenyl deposited in the twisted conformation with λ_{max} ~ 320 nm then red-shifts to 340 nm subsequent to the disorder-to-order transition. Inset: top view.

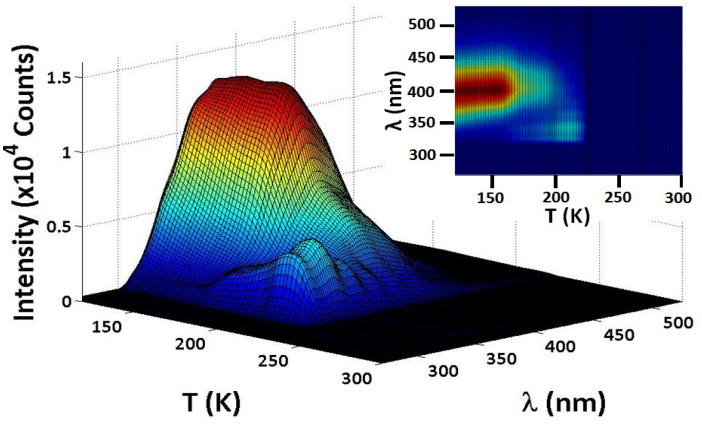

Figure 2. Wavelength-resolved TPD of multilayer 2-ethylnaphthalene. $\Theta_{2\text{-ethylnaphthalene}}$ = 44 ML. The excimer fluorescence at λ_{max} ~ 396 nm dominate at deposition then blue-shifts to 324 nm subsequent to the disorder-to-order transition. Inset: top view.

When multilayer 1-ethylnaphthalene was annealed to 190 K for 30 s, this red-shifted excimer persisted during the 30 s anneal, and reversibly blue-shifted to the 396 nm excimer upon cooling back down to the deposition temperature. After the anneal, the wavelength-resolved TPD showed that 1-ethylnaphthalene underwent a disorder-to-order transition (Figure 4) with the concomitant loss of much of the red-shifted excimer as evidenced by the change from 396 nm with a 3 nm red-shift. A hypothetical model to explain these observations is that the red-shifted excimer that is present at 190 K has sufficient thermal energy to reorient to a geometry that minimized the steric hindrance and is reversibly changed to excimer with λ_{max} ~ 396 nm when the temperature is decreased. During the TPD that followed, the annealed adlayer of 1-ethylnaphthalene underwent the disorder-to-order transition.

Bilayers of 2- and 1-ethylnaphthalene and biphenyl:

Shown in Figures 5 and 6 are the wavelength-resolved TPD of bilayers composed of 2-ethylnaphthalene-biphenyl and 1-ethylnaphthalene-biphenyl, respectively. As noted in the previous section, the ethylnaphthalenes have the lower T_p and were deposited on the bottom, next to the Al_2O_3.

For the 2-ethylnaphthalene-biphenyl bilayer, the self-assembly was immediately apparent upon deposition. The 2-ethylnaphthalene formed with almost no excimer, but instead self-assembled to form exciplexes with the biphenyl when optically excited. This implied that biphenyl was in the planar conformation due to epitaxy and the strong van der Waals interaction between the two molecules. Aggregation-induced emission was about 3-fold. (Figures 2 and 5). Upon reaching the disorder-to-order transition temperature of biphenyl during the TPD experiment, the aggregate became thermally stable. In order to determine the molecular ratio of the exciplex, the fluorescence intensity of the exciplex at about 200 K was plotted as a function of the ratio of coverages of ML biphenyl to ML of 2-ethylnaphthalene in ML ML^{-1}. (Figure 7 in red). At a ratio of about 7±1 ML of biphenyl to ML of 2-ethylnaphthalene coverages, the slope leveled off. This represented the number of biphenyl to 2-ethylnaphthalene in the van der Waals cluster. This number was higher than in biphenyl-naphthalene and biphenyl-methylnaphthalene clusters because of the low symmetry of 2-ethylnaphthalene. The alkyl group in 2-ethylnaphthalene may sterically hinder the formation of a exciplex so that on the average, only 15% of the 2-ethylnaphthalene complexed for every biphenyl molecule and epitaxy occurred only to this limited extent.

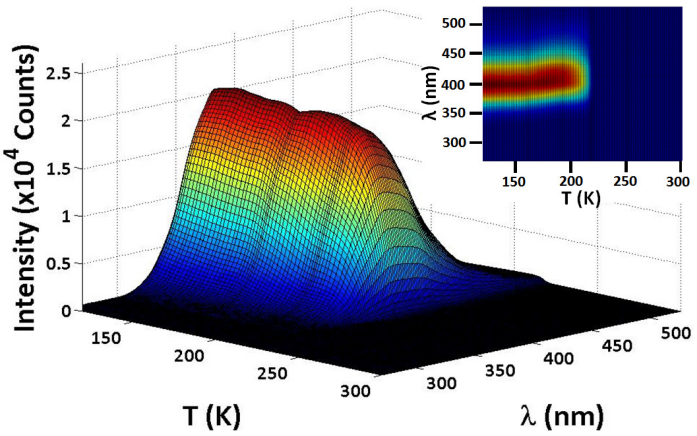

Figure 3. Wavelength-resolved TPD of multilayer 1-ethylnaphthalene. $\Theta_{2\text{-ethylnaphthalene}}$ = 84 ML. The excimer fluorescence at λ_{max} ~ 396 nm dominate at deposition then red-shifts to 400.5 nm. The disorder-to-order transition is not visible. Inset: top view.

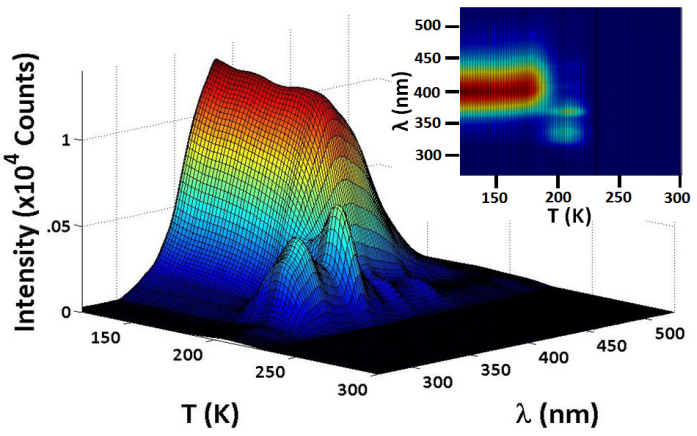

Figure 4. Wavelength-resolved TPD of multilayer 1-ethylnaphthalene. $\Theta_{2\text{-ethylnaphthalene}}$ = 92 ML after annealing at 190 K for 30 s. The excimer fluorescence at λ_{max} ~ 396 nm dominate at deposition then blue-shifts to 324 nm subsequent to the disorder-to-order transition. Inset: top view.

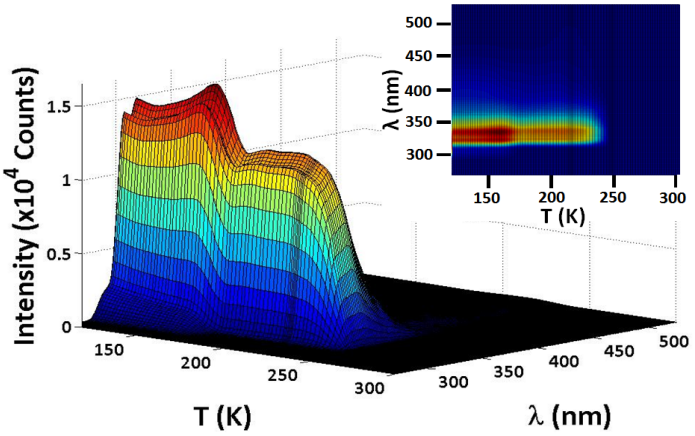

Figure 5. Wavelength-resolved TPD of bilayer of 2-ethylnaphthalene and biphenyl, for which $\Theta_{2\text{-ethylnaphthalene}}$ = 392 ML and $\Theta_{biphenyl}$ = 94 ML. The fluorescence is that of molecular 2-ethylnaphthalene with λ_{max} ~ 324. Note the absence of the 320 nm emission from the twisted conformer of biphenyl. Inset: top view. The biphenyl excimer is barely visible at 370 nm.

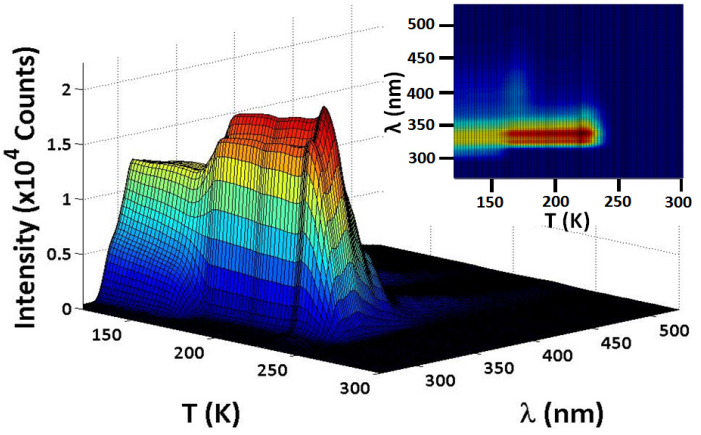

Figure 6. Wavelength-resolved TPD of bilayer of 1-ethylnaphthalene and biphenyl, for which $\Theta_{1\text{-ethylnaphthalene}}$ = 84 ML and $\Theta_{biphenyl}$ = 206 ML. The fluorescence is that of molecular 1-ethylnaphthalene with λ_{max} ~ 324. Note the presence of the 320 nm emission from the twisted conformer of biphenyl. Inset: top view. The biphenyl excimer is barely visible at 370 nm.

For the 1-ethylnaphthalene-biphenyl bilayer, the self-assembly was even more apparent and aggregation-induced emission was better than 10-fold. (Figures 3 and 6). Close examination of Figure 6 showed that biphenyl was present both in the twisted and planar conformer as evidenced by the presence of the 320 nm and 370 nm peaks that correspond to the twisted and planar conformers, respectively. For the latter conformation, the excimer of biphenyl was observed. Fluorescence from the biphenyl excimer and twisted conformer transitioned to the planar conformer when biphenyl underwent the disorder-to-order transition and the fluorescence from the exciplex dominated. When the exciplex intensity was plotted as a function of the ratio of coverages of biphenyl to 1-ethylnaphthalene, the plot began to level off at approximately 4±1 ML ML^{-1}. (Figure 7 in blue)

Since the activation energies for desorption can be calculated from T_p (26-28), the difference in the multilayer T_p and the maximum T_p that result due to the van der Waals interaction can be determined. (Figure 8). For 2- and 1-ethylnaphthalene-biphenyl complexes, T_p's shifted from 56.5 to 59.7 and 55.7 to 58.9 kJ mol^{-1}, respectively. In both cases the difference was 3.2±0.5 kJ mol^{-1}. The last number is the estimated van der Waals energies for 2- and 1-ethylnaphthalene-biphenyl complexes, and is consistent with experimentally obtained van der Waals energies for complexes of such molecules as naphthalene-2-methoxynaphthalene (5.6 kJ mol^{-1}) (29) and the perylene-naphthalene complex (4.2 kJ mol^{-1}) (30).

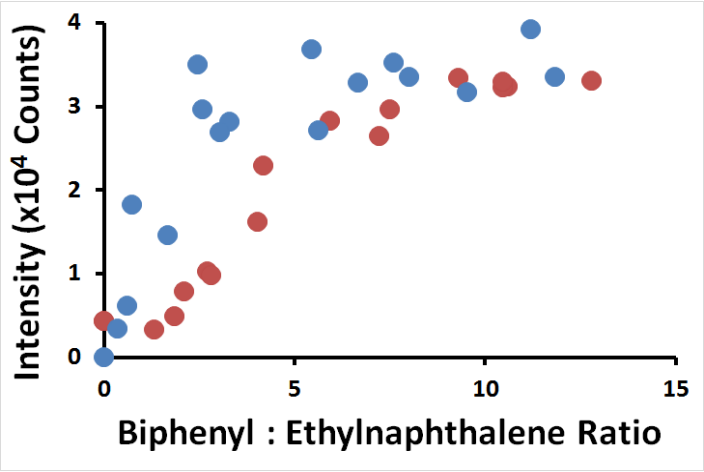

Figure 7. Intensity of the exciplex of 2-ethylnaphthalene peak at 324 nm as a function of the ratio of biphenyl to 2-ethylnaphthalene coverages (ML ML^{-1}) (red) . $\Theta_{2\text{-ethylnaphthalenel}}$ was held constant at 62 ± 18 ML. Intensity of the exciplex of 1-ethylnaphthalene peak at 324 nm as a function of the ratio of biphenyl to 1-ethylnaphthalene coverages (ML ML^{-1}) (blue). $\Theta_{1\text{-ethylnaphthalenel}}$ was held constant at

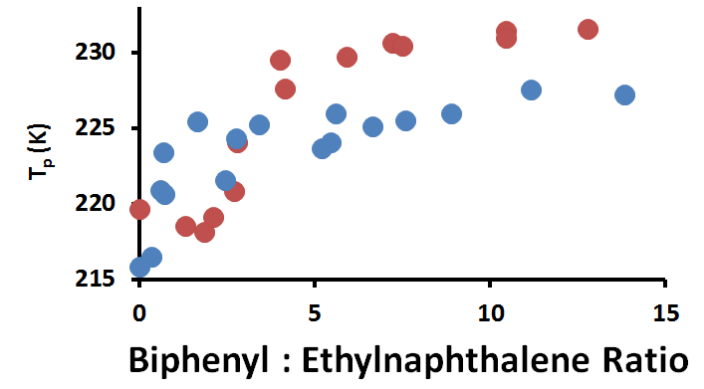

Figure 8. Increase in T_p's for 2-ethylnaphthalene and 1-ethylnaphthalene for bilayers of 2-ethylnaphthalene-biphenyl and 1-ethylnaphthalene-biphenyl, respectively, from mass specific TPD as a function of biphenyl to ethylnaphthalene ratio of coverages (ML ML^{-1}). T_p's for naphthalene (red) with $\Theta_{2\text{-ethylnaphthalene}}$ = 61 ± 14 ML, and T_p's for 1-ethylnaphthalene (blue) with $\Theta_{1\text{-ethylnaphthalene}}$ = 106 ± 13 ML.

In summary, 1- and 2-ethylnaphthalene form van der Waals complex with biphenyl with interaction energies comparable to other naphthalene-biphenyl complexes. Self-assemblage of 2-ethylnaphthalene and biphenyl upon vapor deposition was observed as evidenced by the presistent exciplex during the TPD experiment. Finally, aggregation-induced emission caused a several-fold increase in the normally weak molecular fluorescence in these ethylnaphthalenes.

Acknowledgement

The authors would like to gratefully acknowledge the John Stauffer Charitable Trust for funding the student stipends for summer research.

References

(1). J. Luo, Z. Xie, J.W.Y. Lam, L. Cheng, H. Chen, C. Qiu, H.S. Kwok, X. Zhan, Y. Liu, D. Zhu and B.Z. Tang. *Chem. Commun*. **2001**, 1740-1741.
(2). Y. Hong, J.W.Y. Lam and B.Z. Tang. *Chem Comm*, **2009**, DOI: 10.1039/b904665h
(3). J. Mei, N.L.C. Leung, R.T.K. Kwok, J.W.Y. Lam and B.Z. Tang., *Chem Rev*., **2015**, 115, 11718-11940.
(4). C. Zhu, R.T.K. Kwok, J.W.Y. Lam and B.Z. Tang. *Appl. Bio Mater*. **2018**, 1, 1768-1786.
(5). Z. Liu, Z. Jiang, M. Yan and X. Wang. *Front. Chem*., **2019**, DOI: 10.3389/fchem.2019.00712.
(6). M. Itoh and M. Takamatsu. *Chem. Phys. Lett*., **1990**, 170, 396-400.
(7). R.F.W. Bader, J.R. Cheeseman, K.E. Laidig, K.B. Wiberg and C. Breneman. *J. Am. Chem. Soc*., **1990**, 112, 6530-6536.
(8). R.M. Pitzer, *Acc. Chem. Res*., **1983**, 16, 207-210.
(9). Y.R. Mo and J.L. Gao. *Acc. Chem. Res*., **2007**, 40, 113-119.
(10). S. Liu and N. Govind., *J. Phys. Chem. A*, **2008**, 112, 6690-6699.
(11). L. Goodman, H. Gu, V. Pophristic. *J. Chem. Phys*. **1999**, 110, 4268-4275.
(12). R.S. Mulliken, *J. Chem. Phys*. **1939**, 7, 339-352.
(13). I.B. Berlman. Handbook of Fluorescence Spectra of Aromatic Molecules, 2nd edition, Academic Press, New York, NY (1971) pp.176-177,330.
(14). J.B. Birks. Photophysics of Aromatic Molecules, John Wiley & Sons Ltd., New York, NY (**1970**), pp. 301-370.
(15). Marissa K. Condie, Zackery E. Moreau and A.M. Nishimura. *J. Undergrad. Chem. Res*., **2019**, 18, 15-18.
(16). B.D. Fonda, M.K. Condi, Z.E. Moreau, Z.I. Shih, B. Dionisio, A. Fitts, L. Foltz, K. Nili and A.M. Nishimura. *J. Phys. Chem. C*., **2019**, 123, 26185-26190.
(17). A. Almenningen, O. Bastiansen, L. Fernholt, B.N. Cyvin, S.J. Cyvin and S. Samdal. *J. Mol. Struct*., **1985**, 128, 59-76.
(18). G.P. Charbonneau and Y. Delugeard. *Acta Crystallographica*

B, **1976**, 32, 1420-1423.
(19). G. Friedrich. *J. Phys. Chem. A*, **2002**, 106, 3823-3827.
(20). M.K. Condie, C. Kim, Z.E. Moreau, B. Dionisio, K. Nili, J. Francis, C. Tran, S. Nakaoka and A.M. Nishimura. *J. Undergrad. Chem. Res*., **2020**, 19, 14-17
(21). M.K. Condie, B.D. Fonda, Z.E. Moreau and A.M. Nishimura. *Thin Solid Films*, **2020**, 697, 137823.
(22). S.C. Rosenhagen, C.C. Tran and A.M. Nishimura. *J. Undergrad. Chem. Res*., **2021**, 20, 15-18.
(23). S.R. Gardner, S.W. Simonds, K.A. Martin and A.M. Nishimura, *J. Undergrad. Chem. Res*. **2011**, 10, 170-174.
(24). H.E. Ryan, S. Lau and A.M. Nishimura. *J. Undergrad. Chem. Res*., **2013**, 12, 41-43.
(25). CC. Tran, S.C. Rosenhagen and A.M. Nishimura. Submitted to *J. Undergrad. Chem. Res*.
(26). P.A. Redhead. *Vacuum*, **1962**, 12, 203-211.
(27). F.M. Lord and J.S. Kittelberger. *Surf. Sci.*, **1974**, 43, 173-182.
(28). D.A. King. *Surf. Sci.,* **1975***,* 47, 384-402.
(29). A. Das, K.K. Mahato and T. Chakraborty. *J. Chem. Phys*., **2001**, 114, 6107-6111.
(30). R.J. Babbitt and M.R. Topp. *Chem. Phys. Lett.*, **1986**, 127, 111-117.